

# Masked Autoencoder for Unsupervised Video Summarization

Minho Shim<sup>1</sup>, Taeoh Kim<sup>1</sup>, Jinyung Kim<sup>2</sup>, Dongyoong Wee<sup>1</sup>

<sup>1</sup> NAVER Cloud <sup>2</sup> KAIST

## Abstract

Summarizing a video requires a diverse understanding of the video, ranging from recognizing scenes to evaluating how much each frame is essential enough to be selected as a summary. Self-supervised learning (SSL) is acknowledged for its robustness and flexibility to multiple downstream tasks, but the video SSL has not shown its value for dense understanding tasks like video summarization. We claim an unsupervised autoencoder with sufficient self-supervised learning does not need any extra downstream architecture design or fine-tuning weights to be utilized as a video summarization model. The proposed method to evaluate the importance score of each frame takes advantage of the reconstruction score of the autoencoder’s decoder. We evaluate the method in major unsupervised video summarization benchmarks to show its effectiveness under various experimental settings.

## 1 Introduction

Video summarization is the task of distilling a long video into a shorter form. For the distillation, each frame needs to be scored based on its importance in the context of the video. Since the definition of importance is subjective, several properties have been considered, including diversity, representativeness, and hierarchical information (Zhou, Qiao, and Xiang 2018; Li et al. 2018, 2021; Jung et al. 2020; Zhao, Li, and Lu 2017). These heuristic properties are induced with several corresponding losses and a mixture of them, transforming visual features into importance scores. We question whether any robust and fully data-driven representation exists that imposes minimal heuristic properties.

Seeking robust representation, unsupervised autoencoders for video summarization were naturally proposed (Yang et al. 2015). The hypothesis behind the unsupervised autoencoders is that videos in a specific domain share similar scenes, and similar parts are scored as highlights. The autoencoders are still confined to the target domain, meaning we need a separate model for each domain of videos. Such limitations of previous unsupervised learning methods gave rise to the need for self-supervised learning (SSL) in both image (Chen et al. 2020; He et al. 2020; Grill et al. 2020; He et al. 2022; Bao, Dong, and Wei 2021) and video (Han, Xie, and Zisserman 2020; Feichtenhofer et al. 2021; Wang et al. 2021; Wei et al. 2022) domains, triggering large-scale backbones’ development. As neither an explicit classifier nor a

class label are used to train SSL models, one can expect SSL models to be more versatile for various downstream tasks. However, the downstream tasks in the video domain is limited when excluding classification-based tasks like video action recognition, compared to natural language processing and image understanding (Sec. 2.2). As no work has researched how the self-supervised knowledge of features affects unsupervised video summarization (Apostolidis et al. 2021), we expand the topic to the video summarization task, which is a temporally dense understanding task.

In the video summarization task, some experimental settings have sufficient room to be diversified. Existing unsupervised methods mostly use the videos in the target domain for training by splitting the target summarization dataset (Jung et al. 2019; Apostolidis et al. 2021). Alongside recent claims on the necessity of transition to new evaluation metrics (Otani et al. 2019; Apostolidis et al. 2020a), we discovered that cross-validation with split datasets in the community is not standardized and can affect each model’s performance. If a method were completely unsupervised by being agnostic to the target dataset, we could use summarization datasets as a whole for evaluation.

To this end, we propose to fuse a strong SSL backbone and video summarization. Fig. 1(a) shows existing approaches that concatenate backbone models for feature extraction and separate downstream models. In contrast, our proposed method does not require any separate summarization model, but a single autoencoder is capable of both understanding and measuring the importance score of each video frame, as shown in Fig. 1(b). Our autoencoder is built as a variant of masked autoencoders (He et al. 2022; Bao, Dong, and Wei 2021). Recent research on masked autoencoders uses the decoder only for SSL pretraining stage, and the encoder is used alone for feature extraction or fine-tuning on video downstream tasks. On the other hand, we propose a simple computation of decoder outputs to calculate the dissimilarity of a reconstructed frame against its original input. Then, the dissimilarity is used as a score for evaluating each frame as a summary or not. The process makes the proposed method completely unsupervised, i.e., labels are not used for pretraining and fine-tuning is not needed, thus the model is agnostic to summarization datasets.

The effectiveness and simplicity of the proposed method are demonstrated in unsupervised video summarization

benchmarks with minimal hyperparameters and without bells and whistles. In addition, extensive experiments are provided to discover which aspects of pretrained video representation affect summarization quality.

In summary, our methodological, integrative, and empirical contributions are as follows:

- We re-introduce autoencoder for unsupervised video summarization, with complete target domain-agnostic characteristics.
- To our knowledge, we provide the first bridge between self-supervised learning and video summarization.
- Extensive experiments show how choices of parameters and training settings (unsupervised fine-tuning or cross-dataset validation) affect the model’s effectiveness.

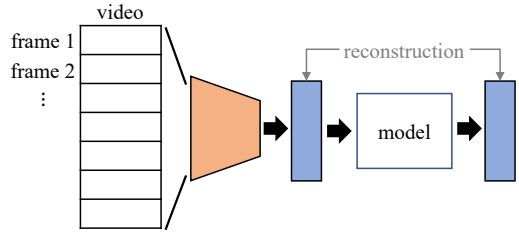
## 2 Related Work

### 2.1 Video Summarization

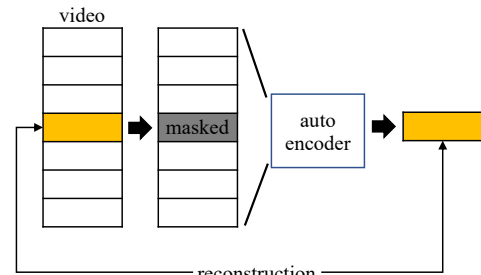
Unlike supervised learning-based deep video summarization that requires summary annotations provided by humans (Zhang et al. 2016; Fajtl et al. 2018; Zhao, Li, and Lu 2017; Rochan, Ye, and Wang 2018; Zhang, Grauman, and Sha 2018; Zhao, Li, and Lu 2018; Park et al. 2020; Saquil et al. 2021; Chen et al. 2022), unsupervised learning-based approaches have been proposed and received attention because human annotations are too subjective and expensive. Zhou et al. (2018) propose a reinforcement learning-based framework whose reward is based on the diversity and representativeness of the summarized video. Another important stream of unsupervised video summarization research is to reconstruct or generate video summaries using autoencoders or generative models. Yang et al. (2015) first proposed autoencoder-based unsupervised video summarization. Following advances in adversarial learning (Goodfellow et al. 2014) for various vision applications, Mahasseni et al. (Mahasseni, Lam, and Todorovic 2017) propose generators to select summary frames, and the discriminator distinguishes between the original video and the reconstructed video from summary frames. Following works have enhanced (Mahasseni, Lam, and Todorovic 2017) using two-stream networks with regularization loss (Jung et al. 2019), bi-directional generative models using cycle-consistency loss (Yuan et al. 2019), or generative model learning from the unpaired videos (Rochan and Wang 2019). Some works have focused on enhancing the model structure using attention mechanisms (He et al. 2019; Apostolidis et al. 2020b; Jung et al. 2020). Our contributions do not reside in architectural choices. Instead, we are the first to propose a simple method to use autoencoders in a self-supervised framework for solving the video summarization task.

### 2.2 Self-supervised Learning

Visual self-supervised representation learning methods (Chen et al. 2020; He et al. 2020; Misra and Maaten 2020; Grill et al. 2020) recently received much attention and are based on the instance discrimination (Wu et al. 2018) that learns invariance between semantically positive samples using data augmentation. This concept is extended



(a) Separate backbone and summarization model.



(b) Integrated backbone.

Figure 1: Comparison between separate backbone with summarization model, and the integrated autoencoder model. (a) shows a horizontal concatenation of the video representation network and a summarization model. The weights of the representation network is usually pretrained and fixed, and the impact of the representation is yet deeply explored. In (a), *reconstruction* is written in gray color to indicate it is applied when the model is an autoencoder (Yang et al. 2015). Our proposed method (b) uses a single autoencoder for both pretraining and summary score prediction.

to the video domain (Han, Xie, and Zisserman 2020; Chen et al. 2021; Qian et al. 2021; Feichtenhofer et al. 2021; Recasens et al. 2021; Wang et al. 2022). From the perspective of downstream tasks, image SSL has extended to object detection, segmentation (Wang et al. 2021; Roh et al. 2021; Hénaff et al. 2021), or multi-modal tasks (Huang et al. 2021; Kim, Son, and Kim 2021) combined with natural language processing which has more diverse downstream tasks (Wang et al. 2019). In contrast, in the video domain, the scope of downstream tasks does not deviate significantly from action recognition (Soomro, Zamir, and Shah 2012; Kuehne et al. 2011) (some studies have included fine-grained action recognition (Gu et al. 2018; Shao et al. 2020)). Recently, there has been increasing interest in masked target prediction-based SSL in the image domain (He et al. 2022; Bao, Dong, and Wei 2021; Dong et al. 2021; Xie et al. 2022) and video domain (Wei et al. 2022). These methods have not only shown promising performances compared to the instance discrimination but also opened up the possibilities of new tasks beyond recognition. Inspired by this, we propose to naturally connect the autoencoder-based method of unsupervised video summarization.

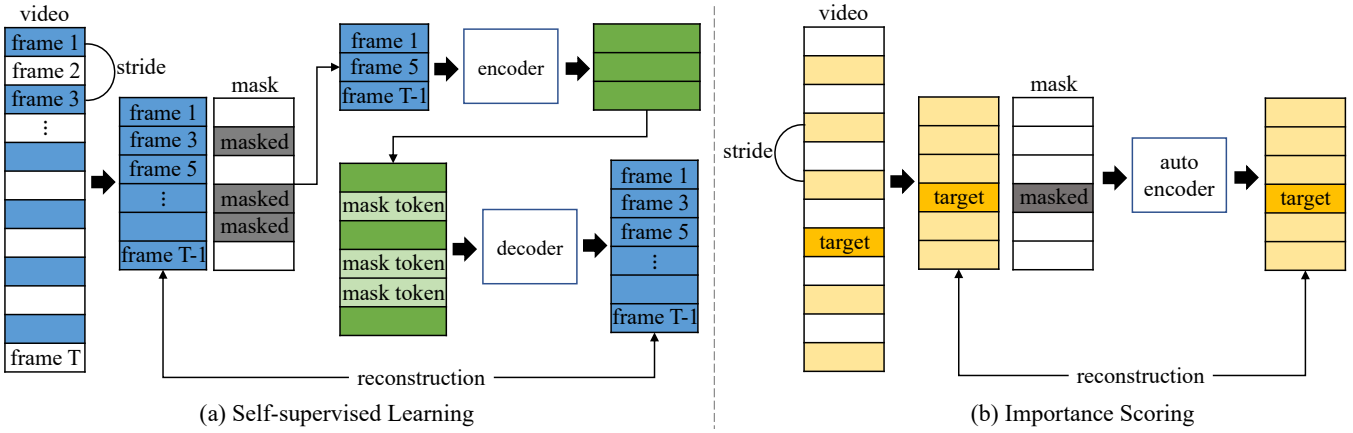


Figure 2: Design of frameworks for (a) self-supervised learning and (b) importance scoring of video summarization. In this figure, the temporal stride for frame sampling is set as 2 for example. For SSL, stride is applied based on a random starting frame. For summarization, stride is applied based on the target frame set as a center frame.

### 3 Approach

Our approach employs autoencoders for reconstructing frames and uses the reconstruction to determine the importance score of the frame. The superficial concept is the same as the previous work using autoencoder for unsupervised video summarization (Yang et al. 2015), but details are distinct in multiple aspects. Early usage of the autoencoder is to find a latent space that commonly represents a given video’s domain. For example, in swimming videos, parts of videos containing the actual swimming motion are the most commonly found visual information in the videos. Other activities are expected to be regarded as redundant parts and to be discarded. Previous approaches (Yang et al. 2015) encode and decode video segments, searching for common segments found in each specific domain of videos.

Our model instead reconstructs a single target frame within a context of other frames. Those other frames can be neighbors right next to the target or far from the target. No matter the context, the autoencoder is expected to understand the relationship between the frames and reconstruct the masked target frame.

We propose a framework suitable for video self-supervised learning (SSL) and video summarization. The autoencoder-based SSL itself is not our invention. We rather bridge the gap in the model architecture between the self-supervised pretraining stage and the downstream summarization task. Existing downstream video tasks of SSL require an extra design of the head architecture built upon the SSL-trained backbone. Also, the decoder is mostly discarded in the downstream video tasks. Considering the cost of SSL training, reusing the decoder in the downstream task is beneficial as it has a degree of expressive power. In order to achieve this, we introduce the method of directly using the SSL-trained encoder and decoder for summarization.

#### 3.1 Data Preprocessing

Video summarization task naturally deals with long videos. To reduce computation and memory usage, using one-

dimensional features is conventional, extracted from each frame or segment of videos. Popular choices are two-dimensional (2D) convolutional neural networks (CNN) followed by recurrent neural networks like LSTM (Apostolidis et al. 2021). We use 2D CNN pretrained on ImageNet to extract 1D features from all frames of videos in datasets for self-supervised learning and downstream summarization. We do not reduce video frames per second (fps), in contrast to the recent video summarization research (Zhang et al. 2016; Zhou, Qiao, and Xiang 2018; Saquil et al. 2021; Jung et al. 2019, 2020).

#### 3.2 Architecture

Since an attention-based architecture dubbed transformer has been proposed in natural language processing (Vaswani et al. 2017), masked token prediction popularized the usage of the transformer architecture (Devlin et al. 2019). This effort continues in computer vision by introducing vision transformers (ViT) in the image domain (Dosovitskiy et al. 2021) and its variants in the video domain (Fan et al. 2021; Liu et al. 2021). Both encoder and decoder in our autoencoders are built upon the transformer (Devlin et al. 2019; Dosovitskiy et al. 2021). As our input is one-dimensional, the linear projection for patch embedding in ViT is not needed, while sinusoidal positional embedding is directly applied to the input sequence of frames.

#### 3.3 Self-supervised Learning

Following the recent masked target prediction-based SSL model (He et al. 2022), we build an SSL model suitable for video summarization tasks with an adaptation of asymmetric encoder-decoder design. The asymmetry means the encoder only encodes unmasked frames, while the decoder both sees encoded frames with masked frames. Fig. 2(a) shows the process of SSL. Given a sequence of frames, we randomly mask a fixed ratio of frames in the sequence. Then, the encoder encodes the unmasked frames with positional embedding. The output of the encoder is concatenated with masked

SSL	summ.	$\tau$	$\rho$	SSL	summ.	$\tau$	$\rho$		
1	1	0.105	0.138	<i>rand(1,4)</i>	1	0.108	0.142		
1	2	0.105	0.138	<i>rand(1,4)</i>	2	0.108	0.142		
1	3	0.104	0.137	<i>rand(1,4)</i>	3	0.107	0.140		
1	4	0.103	0.135	<i>rand(1,4)</i>	4	0.105	0.138		
2	1	0.107	0.141	<i>rand(1,8)</i>	2	0.110	0.144		
2	2	0.107	0.142	<i>rand(1,8)</i>	4	0.106	0.140		
2	3	0.106	0.140	<i>rand(1,8)</i>	6	0.103	0.136		
2	4	0.104	0.137	<i>rand(1,8)</i>	8	0.101	0.133		
(a) Fixed training stride.				(b) Random training stride.					
ratio	$\tau$	$\rho$	feature	model	$\tau$	$\rho$	#ep	$\tau$	$\rho$
0.10	0.109	0.144	ResNet-50	base	0.084	0.110	200	0.110	0.144
0.30	0.109	0.143	<u>GoogLeNet</u>	<u>base</u>	0.110	0.144	400	0.109	0.143
<u>0.50</u>	0.110	0.144	ResNet-50	large	0.083	0.110	600	0.109	0.144
0.70	0.108	0.142	GoogLeNet	large	0.108	0.143	800	0.109	0.143
(c) Mask ratio.				(d) Input feature & model size.				(e) SSL epochs.	

Table 1: Experimental results of analysis. Results in (a)-(e) are trained with self-supervision on MK200 dataset and tested on TVSum dataset. Underlined settings are our defaults. In (a)-(b), “SSL” denotes values used for self-supervised training and “summ.” indicates values used for testing. Higher values of Kendall’s  $\tau$  and Spearman’s  $\rho$  indicate better performance.

tokens, and the order of frames is recovered. The masked tokens consist of learnable parameters, but each mask token is identical. The decoder reconstructs the masked regions with positional embedded inputs, and only the masked frames are used to compute the mean squared error loss.

In this SSL model, we spotlight the temporal *stride* when sampling frames from the video. We suspect the use of different strides is not studied well (Wei et al. 2022). We discovered that a variable use of stride makes the summarization model more robust and flexible to different strides and improves summarization scores. The effect of diverse strides is explored in Sec. 4.4.

### 3.4 Importance Scoring for Summarization

Given the SSL pretrained model, the model directly predicts each video frame’s importance score without additional training. In Fig. 2(b), the *target* is a frame targeted for scoring its importance as a summary frame. We set the target frame to a center frame and retrieve frames around the target frame given a stride parameter. Smaller and larger strides imply local and broad context in the perspective of the target frame. Then, only the target frame is masked and reconstructed by the encoder-decoder of our autoencoder. For every frame in the video, we now have a reconstructed feature and an original frame feature. Importance is scored as a cosine dissimilarity of those two features. The cosine dissimilarity is computed by extracting the cosine similarity of features from 1.

## 4 Experiments

### 4.1 Dataset

For self-supervised learning, we use a video action recognition dataset Mini-Kinetics (MK200) (Xie et al. 2018), by default. MK200 is a balanced subset of Kinetics-400 (K400) (Carreira and Zisserman 2017), decreasing the number of classes from 400 to 200. Alongside K400 and MK200, we also use Kinetics-100 (K100) (Chen et al. 2021) with 100 classes to analyze the model’s scalability. We use MK200 by default because K400 is too large for various ablation studies and parameter searches. As we are using Kinetics for SSL, the labels are not used.

Three benchmark datasets, TVSum (Song et al. 2015), SumMe (Gygli et al. 2014), and FineGym (Shao et al. 2020), are used for video summarization. For TVSum and SumMe, we use the multiple annotated importance frame-level scores as our ground truth, following previous approaches (Otani et al. 2019; Saquil et al. 2021; Apostolidis et al. 2020b). FineGym is originally a fine-grained action recognition dataset, but it was later proposed to be used as a summarization benchmark for longer videos (Saquil et al. 2021). Thus, there is a single summary ground truth for FineGym. Refer to Appendix A1 for dataset properties.

### 4.2 Evaluation

For several years, F1-score evaluation has been dominantly used for video summarization. The F1-score depends on a video temporal segmentation (e.g., KTS (Potapov et al. 2014)) to generate fragments and a key-fragment selection

#samples	base_lr	$\tau$	$\rho$
w/o fine-tuning		0.110	0.144
10,000	4e-4	0.114	0.150
50,000	4e-4	0.113	0.148
10,000	4e-5	0.113	0.149
50,000	4e-5	0.116	0.152

(a) Unsupervised fine-tuning.

SSL Dataset	Test Dataset	TVSum		SumMe		FineGym	
		$\tau$	$\rho$	$\tau$	$\rho$	$\tau$	$\rho$
	TVSum	0.113	0.149	-0.006	-0.007	0.163	0.200
	SumMe	0.011	0.014	0.063	0.077	-0.008	-0.009
	FineGym	0.116	0.153	0.008	0.009	-0.064	-0.079

(b) Cross-dataset validation.

Table 2: Experimental results of (a) unsupervised fine-tuning (Sec. 4.5) and (b) cross-dataset validation (Sec. 4.7). TVSum dataset is used for (a). SSL trained models of each dataset from Table A1 are used for (b).

(e.g., Knapsack) (Apostolidis et al. 2021). Albeit widely used, recent literature started to propose substitutes for the F1-score (Otani et al. 2019; Apostolidis et al. 2020a). We do not mainly report F1-score for the following reasons. First, a random prediction can get a high F1-score comparable with the SoTA unsupervised methods. Second, even a random prediction in some cases can get a higher F1-score than human ground truth (GT) based baseline F1-score. One can suspect F1-score may lack sufficient discrimination between random and human baseline (Otani et al. 2019; Apostolidis et al. 2021).

We use Kendall’s  $\tau$  and Spearman’s  $\rho$  to compare the ground truth scores against our model’s predictions.  $\tau$  and  $\rho$  both measure the association of two different ranked data, and they are proposed (Otani et al. 2019) to be used for the evaluation of video summarization.  $\tau$  and  $\rho$  are started to be used on the TVSum dataset (Jung et al. 2020), and the usage is expanded over the SumMe and FineGym dataset (Saquil et al. 2021). These rank-based metrics can clearly discriminate between random and human baseline, as random predictions get zero scores and the human GT gets high scores (Table 3). We meticulously follow Saquil et al. (2021), and use public codes and data for evaluation.

Furthermore, as our method is agnostic to the target domain dataset, training and evaluation do not require splitting data for cross-validation. This agnostic property is beneficial because many unsupervised methods in the bibliography do not publicly open their splits, i.e., each work uses a different set of videos for cross-validation. We simulate 5-split validation in Appendix A3.2, and the results show that using a unified set or using the entire dataset like ours is crucial for a fair comparison. Additionally, in Appendix A3.1, we share F1-scores of our models only for reference but not as our primary evaluation.

### 4.3 Implementation details

We extract features from video frames using ResNet-50 (He et al. 2016) or GoogLeNet (Szegedy et al. 2015), both pre-trained on ImageNet (Deng et al. 2009), resulting in 2,048 or 1,024 dimensions of input features, respectively. The autoencoder’s encoder and decoder are two ViTs (Dosovitskiy et al. 2021) adopted for temporal features, as mentioned in Sec. 3.2. The number of input frames is 30, and the stride

for temporal frame sampling is set to a fixed value, or the stride is randomly selected for every input sample (Sec 4.4). For example, if the temporal stride is 2, every other frame is sampled over 60 frames. For SSL training, the start frame of a segment is randomly chosen among each video’s temporal dimension with attention to the length of the video, so the end frame does not overflow the length. Additional implementation details are in Appendix A1.

### 4.4 Analysis

In this section, we explore how self-supervised training affects performances of video summarization. Extensive experiments are conducted with different temporal strides (frame sampling rate), masking ratios, input features, and the number of training epochs. Results are shown in Table 1. Underlined settings in each table are used as our default values unless otherwise specified. For example, the mask ratio of 0.50 in Table 1(c) is our default, and then the ratio is used for every other experiment in the other tables. Before inspecting each property, the initial impression of values in Table 1 implies the robustness of self-supervision. Namely, the model is insensitive to the changes in the parameters.

**Temporal stride.** In Table 1(a), models are trained with a fixed value of temporal stride of 1 or 2. Generally, as the stride used for summarization gets deviant from the stride used for training, the performance worsens. When the model is trained with a stride of 2 and tested with strides of 2 and 4,  $\tau$ s are 0.107 and 0.104, respectively. The results are intuitive as views on each moment become contrasting if different strides are used for training and testing.

Adopting different views on videos using multiple strides is a notable way of teaching machines to understand videos in diverse temporal contexts, e.g., SlowFast (Feichtenhofer et al. 2019) of video action recognition and stride-based instance discrimination (Recasens et al. 2021; Wang et al. 2022). However, training with multiple strides is yet widely studied in the context of masked autoencoders. In pursuit of versatility, we propose randomly selecting a temporal stride for every training sample and letting the model reconstruct masked frames. Even though the model is unaware of the exact stride value, the model is expected to figure out the different temporal ranges of each clip.

In Table 1(b),  $rand(1,4)$  denotes that the stride value is

randomly chosen from 1 to 4 for every self-supervised training sample. The model trained with  $rand(1,8)$  showed better performances than the model with the fixed stride. This implies that a model with more diverse experience in temporal strides can generate better summaries. We selected  $rand(1,8)$  as our default training parameter, and the stride of 2 is used for default testing unless otherwise specified. The reason for using the maximum stride of 8 is detailed in Appendix A1.

**Mask ratio.** The mask ratio determines how much proportion of frames is removed for reconstruction in a training phase. Table 1(c) shows five different mask ratios. Among them, the mask ratio of 0.50 gives the best performance. The worst performing ratio is 0.90. However, this is an interesting observation as the performance drop is only 0.003 in terms of  $\tau$ . Even with most of the frames deleted, the model is capable of learning to reconstruct and generate summaries.

**Input feature and model size.** We test two types of feature extraction models in Table 1(d). ImageNet classification top-1 accuracy of the models (Paszke et al. 2019) are 76.13% and 69.78% respectively for ResNet-50 and GoogLeNet. Even though ResNet-50’s classification performance is higher, we discovered its  $\tau$  and  $\rho$  are significantly smaller than GoogLeNet. With this initial impression, we try a larger model as the ResNet feature is 2048 while the GoogLeNet feature is 1024. However, the increase in model complexity slightly drops the performance for both features. The results suggest that features with higher classification capability are not necessarily beneficial for summarization. At least, the GoogLeNet feature is more suitable for our model, and we use GoogLeNet as our default input feature.

**Model training.** Since SSL does not use any labels, it is hard to determine the duration of training quantitatively. Thus, it is desired for SSL models to be robust to the number of epochs. The robustness means the performance on downstream tasks increases to a certain point and does not decrease even if the model is SSL-trained for more epochs. We tested four different numbers of epochs in Table 1(e). It is worth noting that we use learning rate scheduling and warmup (Appendix A1). The results show our model’s robustness to the number of epochs. Our default 200 epochs experiment gives the best performance, and it is practically maintained even if the number increases up to 800.

## 4.5 Unsupervised Fine-tuning

The ultimate goal of SSL is to build a transdisciplinary model pretrained on a large-scale dataset. Still, our SSL training can be directly applied to the downstream TVSum dataset for unsupervised fine-tuning. This fine-tuning is expected to give priors about the domain of the dataset. This kind of successive SSL training is not common, so the strategy can give interesting observations on whether the second training can boost the summarization performance. We apply the same SSL strategy (Sec. 3.3) to the TVSum dataset. The difference is that videos in TVSum are longer than Kinetics, so there is more room for randomly sampling a clip in the temporal dimension with the same temporal stride.

Method	TVSum		SumMe		FineGym	
	$\tau$	$\rho$	$\tau$	$\rho$	$\tau$	$\rho$
Human	.177	.204	.212	.212	-	-
Random	.000	.000	.000	.000	.000	.000
dppLSTM	.042	.055	-.026	-.031	-.027	-.033
DR-DSN	.020	.026	.043	.050	.146	.178
DR-DSN <sub>2000</sub>	.152	.198	-.016	-.022	NaN	NaN
GANSUM	.024	.032	-.010	-.012	-	-
CSNet	.025	.034	-	-	-	-
GANSUM+AAE	-.047	-.062	-.018	-.023	-	-
GANSUM+GL+RPE	.064	.084	-	-	-	-
CSNet+GL+RPE	.070	.091	-	-	-	-
Ours	.110	.144	.046	.057	.055	.067

Table 3: Results compared to existing unsupervised video summarization methods. Metrics are Kendall’s  $\tau$  and Spearman’s  $\rho$ . Leading zeros are omitted. References for each methods: dppLSTM (Zhang et al. 2016), DR-DSN (Zhou, Qiao, and Xiang 2018), DR-DSN<sub>2000</sub> (Zhou, Qiao, and Xiang 2018; Saquil et al. 2021), GANSUM (Mahasseni, Lam, and Todorovic 2017), CSNet (Jung et al. 2019), GANSUM+AAE (Apostolidis et al. 2020b), and GANSUM/C-SNet+GL+RPE (Jung et al. 2020).

In Table 2(a), “#samples” indicates the number of randomly sampled clips to be masked and reconstructed for SSL. The experiments show that using 10,000 and 50,000 samples both effectively improves the summarization performance. In the case of 50k samples with a base learning rate of 4e-5,  $\tau$  improved by about 5.4%. Since 50k is much smaller than training 200 epochs on MK200, the unsupervised fine-tuning is very effective. Also, the effortless fine-tuning implies that our SSL-trained autoencoder is a well-generalizable model for the summarization task.

## 4.6 Comparison

**Fairness.** Table 3 presents the results of existing unsupervised video summarization methods compared to ours. Since the evaluation metrics have recently become popular, we bring the best values from peer-reviewed papers (Jung et al. 2020; Saquil et al. 2021). In addition, all methods except ours split the dataset for cross-validation (e.g., 5-split) and report the average of the results. Many of them do not publicize the splits, so the settings are different for each method. On the other hand, our method is entirely agnostic to the summarization dataset, so we evaluate our method on all videos without making any splits. The repercussion of using 5-split validation is analyzed in Appendix A3.2.

These multiple differences between methods can make the comparison look unfair. We believe the differences have been accepted considering the subjective characteristic of the video summarization task. As we propose our method as a new wave of video summarization, i.e. as an unsupervised downstream task of SSL, Table 3 is to provide an insight into performances. Note that the model can achieve higher scores under different settings like unsupervised fine-tuning

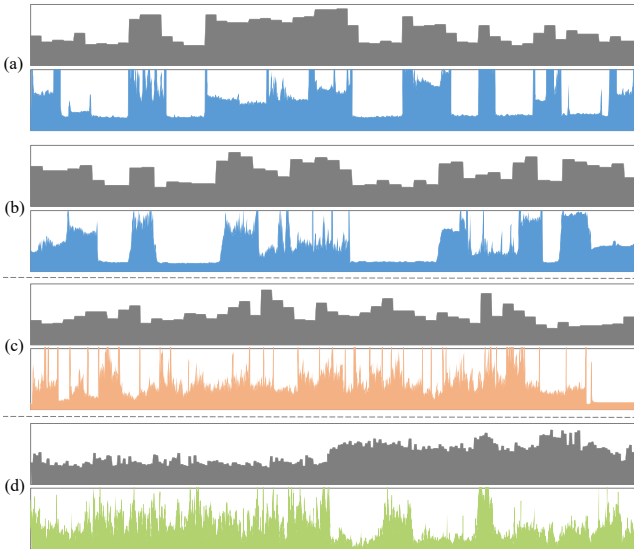


Figure 3: Visualization of ground truth and predicted importance scores. All charts’ x-axis indicate frame number of each video, and y-axis shows scores, appropriately scaled and truncated for the sake of visualization. From (a) to (d), the videos (and video IDs) are video\_5 (XzYM3PFTM4w), video\_38 (EE-bNr36nyA), video\_26 (91IHQYk1IQM), and video\_33 (xmEERLqJ2kU), respectively.

(Sec. 4.5) and cross-dataset training (Sec 4.7).

**Results.** In the TVSum dataset, the most recently proposed method in Table 3 is CSNet+GL+RPE. Our method outperforms CSNet+GL+RPE with gains of 0.040 and 0.053 in  $\tau$  and  $\rho$ , respectively. In the case of the SumMe dataset, it is difficult to tell whether the evaluations are consistent with the TVSum dataset. Three methods, dppLSTM, GAN-SUM, and GANSUM+AAE, show lower values of  $\rho$  than the values of  $\tau$ . This implies that these three methods have large deviations in their ranks’ correlation against ground truth, as Spearman’s  $\rho$  is more sensitive to big deviations than Kendall’s  $\tau$ . In other words, our method and DR-DSN (Zhou, Qiao, and Xiang 2018) can be seen as methods that make fewer large mistakes. DR-DSN is notably inferior in the TVSum dataset, implying less generalization performance. DR-DSN is originally proposed with the default of 60 epochs of training. DR-DSN<sub>2000</sub> is a 2000-epoch trained version of DR-DSN later discovered by Saquil et al. (2021). DR-DSN<sub>2000</sub> gives high scores for TVSum, but it is reported to give unstable results for the others, showing NaN in some cases. On the other hand, our model is robust to the number of training epochs, as shown in Table 1(e).

#### 4.7 Cross-dataset Validation

In Sec. 4.6, we trained the model on Kinetics and tested on three datasets. In the same manner, the model can be SSL trained on one of the three video summarization datasets and tested on each one of them. Table 2(b) shows the results. One interesting outcome is that TVSum and FineGym are mutu-

ally complementary. The model trained on FineGym gives the best result in TVSum testing, even better than the model trained with TVSum, and vice versa for FineGym testing. SumMe dataset does not show any complementary characteristics with the other datasets.

#### 4.8 Visualization

To help understand how our autoencoder-based summarization works, Fig. 3 illustrates our model’s predictions compared to ground truth scores. Each of (a)-(d) is a video from the TVSum dataset, and each has two rows of charts. The first rows with gray charts show ground truth importance scores, averaged over different annotators. Second colored rows are charts of predicted importance scores. (a)-(b) are strong cases, (c) is a moderate, and (d) is a failure case.

In detail, prediction score spikes are often observed to be located at the start and end of high ground truth scored regions. As our predicted importance score is derived from reconstruction dissimilarities, high spikes are often related to shot boundaries or peculiar frames for summarization. In the failure case of (d), it is hard to tell with our predictions which regions are worth to be highlighted, except for some distinctively high-scored parts.

## 5 Conclusion and Future Work

In this paper, we focus on introducing a new paradigm for the video summarization task. We explore how self-supervised autoencoders can be directly used for video summarization without imposing any additional losses, fine-tuning weights, or limiting the target domain. Our proposition is about unsupervised summarization, and supervised summarization as an SSL downstream can be the next step. For the supervised version, it is another research area to explore if our unsupervised models with high summarization performance are aligned with the supervised models’ performance, or if it is aligned with other properties or different downstream tasks like action classification. We hope our proposed framework and analyses will establish a foothold for future work on both SSL and video summarization.

## References

- Apostolidis, E.; Adamantidou, E.; Metsai, A. I.; Mezaris, V.; and Patras, I. 2020a. Performance over random: A robust evaluation protocol for video summarization methods. In *MM*. 1, 5
- Apostolidis, E.; Adamantidou, E.; Metsai, A. I.; Mezaris, V.; and Patras, I. 2020b. Unsupervised video summarization via attention-driven adversarial learning. In *MMM*. 2, 4, 6, 12
- Apostolidis, E.; Adamantidou, E.; Metsai, A. I.; Mezaris, V.; and Patras, I. 2021. Video summarization using deep neural networks: A survey. *Proceedings of the IEEE*. 1, 3, 5
- Bao, H.; Dong, L.; and Wei, F. 2021. BEiT: BERT pre-training of image transformers. *arXiv preprint arXiv:2106.08254*. 1, 2
- Carreira, J.; and Zisserman, A. 2017. Quo Vadis, Action Recognition? A New Model and the Kinetics Dataset. In *CVPR*. 4, 10, 11

- Chen, P.; Huang, D.; He, D.; Long, X.; Zeng, R.; Wen, S.; Tan, M.; and Gan, C. 2021. RSPNet: Relative speed perception for unsupervised video representation learning. In *AAAI*. 2, 4
- Chen, T.; Kornblith, S.; Norouzi, M.; and Hinton, G. 2020. A simple framework for contrastive learning of visual representations. In *ICML*. 1, 2
- Chen, Y.; Guo, B.; Shen, Y.; Zhou, R.; Lu, W.; Wang, W.; Wen, X.; and Suo, X. 2022. Video summarization with u-shaped transformer. *Applied Intelligence*. 2
- Deng, J.; Dong, W.; Socher, R.; Li, L.-J.; Li, K.; and Fei-Fei, L. 2009. ImageNet: A Large-Scale Hierarchical Image Database. In *CVPR*. 5, 10
- Devlin, J.; Chang, M.-W.; Lee, K.; and Toutanova, K. 2019. BERT: Pre-training of deep bidirectional transformers for language understanding. In *NAACL*. 3
- Dong, X.; Bao, J.; Zhang, T.; Chen, D.; Zhang, W.; Yuan, L.; Chen, D.; Wen, F.; and Yu, N. 2021. PeCo: Perceptual Codebook for BERT Pre-training of Vision Transformers. *arXiv preprint arXiv:2111.12710*. 2
- Dosovitskiy, A.; Beyer, L.; Kolesnikov, A.; Weissenborn, D.; Zhai, X.; Unterthiner, T.; Dehghani, M.; Minderer, M.; Heigold, G.; Gelly, S.; et al. 2021. An image is worth 16x16 words: Transformers for image recognition at scale. In *ICLR*. 3, 5
- Fajtl, J.; Sokeh, H. S.; Argyriou, V.; Monekosso, D.; and Remagnino, P. 2018. Summarizing videos with attention. In *ACCV*. 2
- Fan, H.; Xiong, B.; Mangalam, K.; Li, Y.; Yan, Z.; Malik, J.; and Feichtenhofer, C. 2021. Multiscale vision transformers. In *ICCV*. 3
- Feichtenhofer, C.; Fan, H.; Malik, J.; and He, K. 2019. Slow-Fast networks for video recognition. In *ICCV*. 5
- Feichtenhofer, C.; Fan, H.; Xiong, B.; Girshick, R.; and He, K. 2021. A large-scale study on unsupervised spatiotemporal representation learning. In *CVPR*. 1, 2, 10
- Glorot, X.; and Bengio, Y. 2010. Understanding the difficulty of training deep feedforward neural networks. In *AISTATS*. 10
- Goodfellow, I.; Pouget-Abadie, J.; Mirza, M.; Xu, B.; Warde-Farley, D.; Ozair, S.; Courville, A.; and Bengio, Y. 2014. Generative adversarial nets. In *NIPS*. 2
- Goyal, P.; Dollár, P.; Girshick, R.; Noordhuis, P.; Wesolowski, L.; Kyrola, A.; Tulloch, A.; Jia, Y.; and He, K. 2017. Accurate, large minibatch SGD: Training imagenet in 1 hour. *arXiv preprint arXiv:1706.02677*. 10
- Grill, J.-B.; Strub, F.; Altché, F.; Tallec, C.; Richemond, P.; Buchatskaya, E.; Doersch, C.; Avila Pires, B.; Guo, Z.; Gheshlaghi Azar, M.; et al. 2020. Bootstrap your own latent-a new approach to self-supervised learning. In *NeurIPS*. 1, 2
- Gu, C.; Sun, C.; Ross, D. A.; Vondrick, C.; Pantofaru, C.; Li, Y.; Vijayanarasimhan, S.; Toderici, G.; Ricco, S.; Sukthankar, R.; et al. 2018. AVA: A video dataset of spatio-temporally localized atomic visual actions. In *CVPR*. 2
- Gygli, M.; Grabner, H.; Riemenschneider, H.; and Gool, L. V. 2014. Creating summaries from user videos. In *ECCV*. 4
- Han, T.; Xie, W.; and Zisserman, A. 2020. Self-supervised co-training for video representation learning. In *NeurIPS*. 1, 2
- He, K.; Chen, X.; Xie, S.; Li, Y.; Dollár, P.; and Girshick, R. 2022. Masked autoencoders are scalable vision learners. In *CVPR*. 1, 2, 3
- He, K.; Fan, H.; Wu, Y.; Xie, S.; and Girshick, R. 2020. Momentum contrast for unsupervised visual representation learning. In *CVPR*. 1, 2
- He, K.; Zhang, X.; Ren, S.; and Sun, J. 2016. Deep residual learning for image recognition. In *CVPR*. 5, 10
- He, X.; Hua, Y.; Song, T.; Zhang, Z.; Xue, Z.; Ma, R.; Robertson, N.; and Guan, H. 2019. Unsupervised video summarization with attentive conditional generative adversarial networks. In *MM*. 2
- Hénaff, O. J.; Koppula, S.; Alayrac, J.-B.; van den Oord, A.; Vinyals, O.; and Carreira, J. 2021. Efficient visual pretraining with contrastive detection. In *ICCV*. 2
- Huang, G.; Sun, Y.; Liu, Z.; Sedra, D.; and Weinberger, K. Q. 2016. Deep networks with stochastic depth. In *ECCV*. 10
- Huang, Z.; Zeng, Z.; Huang, Y.; Liu, B.; Fu, D.; and Fu, J. 2021. Seeing out of the box: End-to-end pre-training for vision-language representation learning. In *CVPR*. 2
- Jung, Y.; Cho, D.; Kim, D.; Woo, S.; and Kweon, I. S. 2019. Discriminative feature learning for unsupervised video summarization. In *AAAI*. 1, 2, 3, 6
- Jung, Y.; Cho, D.; Woo, S.; and Kweon, I. S. 2020. Global-and-local relative position embedding for unsupervised video summarization. In *ECCV*. 1, 2, 3, 5, 6, 12
- Kim, W.; Son, B.; and Kim, I. 2021. Vilt: Vision-and-language transformer without convolution or region supervision. In *ICML*. 2
- Kuehne, H.; Jhuang, H.; Garrote, E.; Poggio, T.; and Serre, T. 2011. HMDB: a large video database for human motion recognition. In *ICCV*. 2
- Li, P.; Ye, Q.; Zhang, L.; Yuan, L.; Xu, X.; and Shao, L. 2021. Exploring global diverse attention via pairwise temporal relation for video summarization. *Pattern Recognition*. 1
- Li, Y.; Wang, L.; Yang, T.; and Gong, B. 2018. How local is the local diversity? Reinforcing sequential determinantal point processes with dynamic ground sets for supervised video summarization. In *ECCV*. 1
- Liu, Z.; Lin, Y.; Cao, Y.; Hu, H.; Wei, Y.; Zhang, Z.; Lin, S.; and Guo, B. 2021. Swin Transformer: Hierarchical vision transformer using shifted windows. In *ICCV*. 3
- Loshchilov, I.; and Hutter, F. 2017. Sgdr: Stochastic gradient descent with warm restarts. In *ICLR*. 10
- Loshchilov, I.; and Hutter, F. 2019. Decoupled weight decay regularization. In *ICLR*. 10

- Mahasseni, B.; Lam, M.; and Todorovic, S. 2017. Unsupervised video summarization with adversarial LSTM networks. In *CVPR*. 2, 6
- Misra, I.; and Maaten, L. v. d. 2020. Self-supervised learning of pretext-invariant representations. In *CVPR*. 2
- Otani, M.; Nakashima, Y.; Rahtu, E.; and Heikkila, J. 2019. Rethinking the evaluation of video summaries. In *CVPR*. 1, 4, 5
- Park, J.; Lee, J.; Kim, I.-J.; and Sohn, K. 2020. Sumgraph: Video summarization via recursive graph modeling. In *ECCV*. 2
- Paszke, A.; Gross, S.; Massa, F.; Lerer, A.; Bradbury, J.; Chanan, G.; Killeen, T.; Lin, Z.; Gimelshein, N.; Antiga, L.; Desmaison, A.; Kopf, A.; Yang, E.; DeVito, Z.; Raison, M.; Tejani, A.; Chilamkurthy, S.; Steiner, B.; Fang, L.; Bai, J.; and Chintala, S. 2019. PyTorch: An Imperative Style, High-Performance Deep Learning Library. In *NeurIPS*. 6, 10
- Potapov, D.; Douze, M.; Harchaoui, Z.; and Schmid, C. 2014. Category-specific video summarization. In *ECCV*. 4
- Qian, R.; Meng, T.; Gong, B.; Yang, M.-H.; Wang, H.; Belongie, S.; and Cui, Y. 2021. Spatiotemporal contrastive video representation learning. In *CVPR*. 2
- Recasens, A.; Luc, P.; Alayrac, J.-B.; Wang, L.; Strub, F.; Tallec, C.; Malinowski, M.; Pătrăucean, V.; Altché, F.; Valko, M.; et al. 2021. Broaden your views for self-supervised video learning. In *ICCV*. 2, 5
- Rochan, M.; and Wang, Y. 2019. Video summarization by learning from unpaired data. In *CVPR*. 2
- Rochan, M.; Ye, L.; and Wang, Y. 2018. Video summarization using fully convolutional sequence networks. In *ECCV*. 2
- Roh, B.; Shin, W.; Kim, I.; and Kim, S. 2021. Spatially consistent representation learning. In *CVPR*. 2
- Saqail, Y.; Chen, D.; He, Y.; Li, C.; and Yang, Y.-L. 2021. Multiple Pairwise Ranking Networks for Personalized Video Summarization. In *ICCV*. 2, 3, 4, 5, 6, 7, 12
- Shao, D.; Zhao, Y.; Dai, B.; and Lin, D. 2020. FineGym: A hierarchical video dataset for fine-grained action understanding. In *CVPR*. 2, 4, 11
- Song, Y.; Vallmitjana, J.; Stent, A.; and Jaimes, A. 2015. Tvsum: Summarizing web videos using titles. In *CVPR*. 4, 11
- Soomro, K.; Zamir, A. R.; and Shah, M. 2012. UCF101: A dataset of 101 human actions classes from videos in the wild. *arXiv preprint arXiv:1212.0402*. 2, 10, 11
- Szegedy, C.; Liu, W.; Jia, Y.; Sermanet, P.; Reed, S.; Anguelov, D.; Erhan, D.; Vanhoucke, V.; and Rabinovich, A. 2015. Going deeper with convolutions. In *CVPR*. 5, 10
- Vaswani, A.; Shazeer, N.; Parmar, N.; Uszkoreit, J.; Jones, L.; Gomez, A. N.; Kaiser, Ł.; and Polosukhin, I. 2017. Attention is all you need. In *NIPS*. 3
- Wang, A.; Singh, A.; Michael, J.; Hill, F.; Levy, O.; and Bowman, S. R. 2019. GLUE: A multi-task benchmark and analysis platform for natural language understanding. In *ICLR*. 2
- Wang, J.; Bertasius, G.; Tran, D.; and Torresani, L. 2022. Long-short temporal contrastive learning of video transformers. In *CVPR*. 2, 5
- Wang, X.; Zhang, R.; Shen, C.; Kong, T.; and Li, L. 2021. Dense contrastive learning for self-supervised visual pre-training. In *CVPR*. 1, 2
- Wei, C.; Fan, H.; Xie, S.; Wu, C.-Y.; Yuille, A.; and Feichtenhofer, C. 2022. Masked feature prediction for self-supervised visual pre-training. In *CVPR*. 1, 2, 4, 10
- Wu, Z.; Xiong, Y.; Yu, S. X.; and Lin, D. 2018. Unsupervised feature learning via non-parametric instance discrimination. In *CVPR*. 2
- Xie, S.; Sun, C.; Huang, J.; Tu, Z.; and Murphy, K. 2018. Rethinking Spatiotemporal Feature Learning: Speed-Accuracy Trade-off in Video Classification. In *ECCV*. 4
- Xie, Z.; Zhang, Z.; Cao, Y.; Lin, Y.; Bao, J.; Yao, Z.; Dai, Q.; and Hu, H. 2022. SimMIM: A simple framework for masked image modeling. In *CVPR*. 2
- Yang, H.; Wang, B.; Lin, S.; Wipf, D.; Guo, M.; and Guo, B. 2015. Unsupervised extraction of video highlights via robust recurrent auto-encoders. In *ICCV*. 1, 2, 3
- Yuan, L.; Tay, F. E.; Li, P.; Zhou, L.; and Feng, J. 2019. Cycle-SUM: Cycle-consistent adversarial LSTM networks for unsupervised video summarization. In *AAAI*. 2
- Zhang, K.; Chao, W.-L.; Sha, F.; and Grauman, K. 2016. Video summarization with long short-term memory. In *ECCV*. 2, 3, 6
- Zhang, K.; Grauman, K.; and Sha, F. 2018. Retrospective encoders for video summarization. In *ECCV*. 2
- Zhao, B.; Li, X.; and Lu, X. 2017. Hierarchical recurrent neural network for video summarization. In *MM*. 1, 2
- Zhao, B.; Li, X.; and Lu, X. 2018. HSA-RNN: Hierarchical structure-adaptive rnn for video summarization. In *CVPR*. 2
- Zhou, K.; Qiao, Y.; and Xiang, T. 2018. Deep reinforcement learning for unsupervised video summarization with diversity-representativeness reward. In *AAAI*. 1, 2, 3, 6, 7

## A1 Implementation Details

**Dataset properties.** Kinetics-400 (K400) is a large-scale human-annotated video action recognition dataset. Each clip contains a single action class, and the duration is around 10 seconds. As the Kinetics dataset consists of public online videos, many of them are unavailable due to expired download links. Except unavailable videos, our K400, Mini-Kinetics-200, and Kinetics-100 contain 241,567, 77,157, and 30,570 videos for SSL training respectively.

TVSum has 50 videos, each containing 7,047 frames on average, and the score is human-annotated with an importance score by 20 different annotators. Annotators give scores to every 2-second-long shot, and the score is applied to every frame in each shot. The score is an integer scale from 1 to 5. SumMe has 25 videos with 4,393 frames on average per video, and the importance score is annotated for each pre-defined shot by 15 to 18 annotators. Every frame within a shot annotated as summary is scored 1, and the other frames are scored 0. For FineGym, selected 50 videos have 231,603 frames on average, and the longest video spans up to 4 hours. Segments annotated as *event* timestamps are marked 1 as summary and 0 otherwise.

**Feature extraction.** Each video frame is resized to  $256 \times 256$ , center-cropped to  $224 \times 224$ , and normalized with ImageNet (Deng et al. 2009) statistics following standard practices (Paszke et al. 2019). Then the images are forwarded with ResNet-50 (He et al. 2016) and GoogLeNet (Szegedy et al. 2015). Lanczos resampling is used for image resizing.

**Model.** The encoder has 12 stacked transformer blocks, each with 12 heads for multi-head attention. The decoder has 4 blocks, each with 6 heads. The embedding dimension of the encoder and the decoder’s attention are 768 and 384, respectively, and the embedding dimension of MLP in each block is 4 times bigger than the embedding dimension of attention (MLP ratio of 4). Compared to the default base model, the large model (Table 1(d)) has bigger embedding dimensions of 1024 and 512 for the encoder and decoder, respectively. On top of that, the encoder has 24 stacked transformer blocks with 16 heads for multi-head attention, and the decoder has 8 blocks, each with 16 heads.

**Self-supervised learning.** AdamW (Loshchilov and Hutter 2019) is used as an optimizer, the base learning rate is set to 4e-4, and linear learning rate scale rule (Goyal et al. 2017) ( $lr = base\_lr \times batch\_size/256$ ) is applied alongside with 40 epochs of warmup. Cosine learning rate schedule (Loshchilov and Hutter 2017) is applied, and the learning rate drops to 1e-6 in the last epoch. We do not use drop-path (Huang et al. 2016) or gradient clipping, and all transformer blocks are initialized with Xavier uniform (Glorot and Bengio 2010). Our default batch size is 128, and self-supervised training is done through 400 epochs. The main reason for limiting the maximum stride value to 8 is that the Kinetics training dataset consists of 10-second videos with an average frame per second (fps) of 27.45. Since we sample 30 frames, a stride of 8 is a safe value. For summarization, the default stride is 2 for every experiment except SumMe, which uses the stride of 31.

**Unsupervised fine-tuning.** We experimented with two different base learning rates. One is our default, 4e-4, and the other is 4e-5. The batch size is 128, so the practical base learning rates are 2e-4 and 2e-5 by the linear scale rule.

All three video summarization benchmarks have at most 50 videos. This means a single clip sampled from each video cannot fill up our default batch size of 128. For training efficiency, we sample 10 clips from each video for every training iteration. As mentioned in Sec. 4.5, this is feasible since videos for summarization are much longer than Kinetics (Carreira and Zisserman 2017). The same strategy is identically applied for self-supervised learning (SSL) on summarization benchmark datasets, explained in the following Sec. A2.2. Additionally, the number of warmup epochs is decreased to 5 in the case of unsupervised fine-tuning.

**Video action recognition.** We describe the training procedure of downstream video action recognition explored in Sec. A2.1. For fine-tuning and inference, the autoencoder’s decoder is replaced with a single fully-connected layer. The layer receives a temporally average-pooled encoder’s output and yields class probabilities. All parameters of the encoder and the fully-connected layer are updated. We train the model with a base learning rate of 0.001, without the linear learning rate scale rule (Goyal et al. 2017). AdamW (Loshchilov and Hutter 2019) is used as an optimizer, with betas of (0.9, 0.999) and weight decay of 0.05. The cosine learning rate schedule (Loshchilov and Hutter 2017) is applied with 5 warmup epochs. The number of action recognition training epochs is 100. For testing, we temporally sample 4 clips from each video uniformly in the temporal dimension, and the results are averaged for action recognition.

**Environment.** We use one to eight NVIDIA A100 GPUs for training and validation. In addition, PyTorch (Paszke et al. 2019) library is used to build and test our architectures.

## A2 Additional Analysis

### A2.1 Correlation with Video Action Recognition

Research on video SSL treats video action recognition as a central downstream task, and the action classification performance is exploited to measure how well the knowledge provided by SSL transfers to other tasks (Feichtenhofer et al. 2021; Wei et al. 2022). In order to explore if the higher action recognition scores lead to good summarization outcomes, we performed action recognition experiments on our model. We conduct supervised fine-tuning on 1-D extracted UCF101 (Soomro, Zamir, and Shah 2012) and measure split-1 accuracy.

Table A2(a) shows recognition top-1 and top-5 accuracy with different mask ratios. In the case of summarization, Table 1(c) presented the ratio of 0.50 as the best even though the gap is small compared to other choices. Action recognition accuracy, however, shows an apparent drop of top-1 accuracy in ratios except 0.30. This reveals that the recognition power does not linearly imply the power of other tasks, summarization in this case. Table A2(b) presents the scalability of the model. Action recognition accuracy increases as

ratio	top-1	top-5
0.10	71.32	89.21
0.30	73.72	90.30
0.50	72.09	89.58
0.70	72.11	89.72
0.90	72.11	88.29

(a) Mask ratio.

dataset	top-1	top-5	$\tau$	$\rho$
Kinetics-100	71.40	88.40	0.110	0.144
Mini-Kinetics-200	72.09	89.58	0.110	0.144
Kinetics-400	73.33	90.72	0.108	0.142

(b) SSL training dataset.

Table A2: Experimental analysis of relationship between video action recognition and video summarization. TVSum dataset is used for these analyses.

#samples	$\tau$	$\rho$	top-1	top-5
100,000	0.096	0.126	68.75	86.33
200,000	0.109	0.143	67.72	85.41
400,000	0.113	0.149	66.77	85.46
600,000	0.112	0.147	67.59	86.20

(a) TVSum.

#samples	$\tau$	$\rho$	top-1	top-5
50,000	0.056	0.068	70.39	88.87
100,000	0.063	0.077	69.89	88.16
200,000	0.059	0.073	70.39	88.87
300,000	0.059	0.072	69.97	88.34

(b) SumMe.

#samples	$\tau$	$\rho$	top-1	top-5
100,000	-0.125	-0.154	71.56	88.69
200,000	-0.099	-0.122	69.73	87.95
400,000	-0.078	-0.096	69.36	88.13
600,000	-0.064	-0.079	69.10	87.89

(c) FineGym.

Table A1: Experimental results of conducting self-supervised learning on target domain dataset (Appendix A2.2). Summarization evaluation metrics are Kendall’s  $\tau$  and Spearman’s  $\rho$ . Action recognition evaluation metrics are UCF-101 (Soomro, Zamir, and Shah 2012) split-1 top-1 and top-5 accuracy.

the size of the dataset rises from K100 to K400. In contrast,  $\tau$  and  $\rho$  stay about the same regardless of the size. We cannot decisively argue which SSL model is better with these results, but they provide initial insights into using the same backbone for diverse video understanding tasks. Therefore, our simple but effective design of unsupervised video summarization can be another tool to find a balance between various tasks’ performances.

## A2.2 Self-supervision on Target Domain Dataset

In the self-supervised part, we mainly used the Kinetics (Carreira and Zisserman 2017) dataset as it is the de facto standard for video SSL pretraining (Sec. 2.2). For video summarization, three benchmark datasets are employed. Instead, in this section, we first SSL train the model directly on video summarization datasets. Then, the trained model is tested on the other datasets in Sec. 4.7, e.g., a model trained on TVSum (Song et al. 2015) is tested on FineGym (Shao et al. 2020).

Unsupervised fine-tuning on the target domain dataset is explored in Sec. 4.5. As the method is fully unsupervised, the training scheme can be directly applied to the video summarization dataset without pretraining on Kinetics. Since the models are trained from scratch, we increase the number of training samples, and the number of warmup epochs is set to 40. We also conduct the same UCF-101 action recognition benchmark (Sec. A2.1).

The results are presented in Table A1. In the case of unsupervised training on the TVSum dataset in Table A1(a), the summarization results reach their peak with 400k training samples and decrease with more samples. However, action recognition top-1 accuracy is the worst with 400k samples. Even the model with the best recognition accuracy is far inferior to models trained with Kinetics. These results suggest the importance of the size and diversity of the dataset in the SSL training phase. When trained on the SumMe dataset, the mean  $\tau$  values are lower, and the mean  $\rho$  values are bigger than the model trained on the Kinetics dataset.

Among three different datasets, FineGym (Shao et al. 2020) showed the best action recognition top-1 accuracy when trained with 100k samples (Table A1(c)). This is reasonable as FineGym is at first proposed as a fine-grained action recognition dataset. In contrast, the recognition accuracies slowly decrease as training samples increase. Summarization scores are in the opposite situation, as  $\tau$  and  $\rho$  are both showing negative scores.

## A3 Supplementary Results

### A3.1 F1-Score

Table A3 shows the key-fragment-based F1-score evaluation with different pretraining datasets. In Sec. 4.2, we mentioned why we do not use F1-score evaluation. Alongside recent trends of changing evaluation metrics (some papers do not

Pretraining Dataset	TVSum	SumMe
MK200	55.1	41.8
TVSum	56.2	42.7
SumMe	54.8	40.6
FineGym	55.2	40.7

Table A3: F1-scores with different pretraining datasets. Beside MK200, refer to Appendix A2 for pretraining settings. FineGym does not have public data for F1-score computation.

Split	TVSum			SumMe			FineGym		
	$\tau$	$\rho$	f1	$\tau$	$\rho$	f1	$\tau$	$\rho$	
Ours	.129	.170	55.8	.028	.035	40.0	.068	.084	
AAE	.096	.126	55.9	.062	.076	46.1	-	-	

Table A4: Results with random 5-split test sets. Leading zeros are omitted to save space. AAE (Apostolidis et al. 2020b) has no splits for FineGym.

report F1-score at all) (Jung et al. 2020; Saquil et al. 2021), we report these values only for references.

### A3.2 Random 5-split

As our default method is self-supervised and agnostic to target domain datasets, we use the entire benchmark datasets for evaluation. On the other hand, previous unsupervised methods split dataset for both training and evaluation. The concern is that only a few previous works publicized their splits, and the others do not specify which set is used for evaluation. It means each work is likely to use a different set of videos for training and evaluation. In Table A4, we compare how random splits can affect the results. We make our own random splits (*Ours* in the table) and bring publicly available sets from AAE (Apostolidis et al. 2020b). We would like to ensure that we only ran the code for random sampling five times to obtain the five splits of TVSum, SumMe, and FineGym, respectively specified in Listing A1, A2, and A3.

Using our default model, we simulate the 5-split evaluation. The results in Table A4 show that randomness severely affects the evaluation. Compared to *Ours* in Table 3, using the entire set for evaluation, results are very variable. Even if the community shares a specific set for evaluation, it may still be an unfair comparison as each method can have different set that the method works well. Also, F1-scores fail to show any performance difference in TVSum. This analysis further strengthens the value of our proposed unsupervised and target dataset-agnostic method.

Listing A1: Our 5-split for TVSum

---

```

1 Split 1:
2   video_35
3   video_23
4   video_15
5   video_40
6   video_12
7   video_29
8   video_21
9   video_28
10  video_22
11  video_6
12 Split 2:
13  video_8
14  video_5
15  video_22
16  video_32
17  video_49
18  video_41
19  video_21
20  video_38
21  video_17
22  video_15
23 Split 3:
24  video_7
25  video_41
26  video_5
27  video_18
28  video_34
29  video_23
30  video_24
31  video_37
32  video_49
33  video_10
34 Split 4:
35  video_14
36  video_38
37  video_16
38  video_3
39  video_39
40  video_2
41  video_46
42  video_8
43  video_49
44  video_36
45 Split 5:
46  video_30
47  video_16
48  video_32
49  video_39
50  video_9
51  video_24
52  video_42
53  video_21
54  video_20
55  video_44

```

---

---

**Listing A2: Our 5-split for SumMe**

---

```
1 Split 1:  
2   video_25  
3   video_5  
4   video_23  
5   video_20  
6   video_11  
7 Split 2:  
8   video_12  
9   video_10  
10  video_22  
11  video_7  
12  video_15  
13 Split 3:  
14  video_6  
15  video_13  
16  video_16  
17  video_18  
18  video_15  
19 Split 4:  
20  video_7  
21  video_21  
22  video_2  
23  video_14  
24  video_16  
25 Split 5:  
26  video_12  
27  video_17  
28  video_16  
29  video_22  
30  video_18
```

---

---

**Listing A3: Our 5-split for FineGym**

---

```
1 Split 1:  
2   video_12  
3   video_29  
4   video_30  
5   video_26  
6   video_20  
7   video_8  
8   video_27  
9   video_40  
10  video_36  
11  video_6  
12 Split 2:  
13  video_22  
14  video_27  
15  video_23  
16  video_5  
17  video_12  
18  video_13  
19  video_21  
20  video_44  
21  video_9  
22  video_11  
23 Split 3:  
24  video_30  
25  video_10  
26  video_32  
27  video_27  
28  video_16  
29  video_25  
30  video_21  
31  video_15  
32  video_22  
33  video_43  
34 Split 4:  
35  video_5  
36  video_36  
37  video_45  
38  video_44  
39  video_7  
40  video_4  
41  video_14  
42  video_42  
43  video_22  
44  video_48  
45 Split 5:  
46  video_3  
47  video_32  
48  video_35  
49  video_18  
50  video_11  
51  video_50  
52  video_7  
53  video_41  
54  video_34  
55  video_8
```

---